



## ORIGINAL ARTICLE

# Case-only design identifies interactions of genetic risk variants at *SIGLEC5* and *PLG* with the lncRNA *CTD-2353F22.1* implying the importance of periodontal wound healing for disease aetiology

Ricarda Müller<sup>1</sup> | Sandra Freitag-Wolf<sup>2</sup> | January Weiner 3rd<sup>3</sup> |  
Avneesh Chopra<sup>1</sup> | Tugba Top<sup>1</sup> | Henrik Dommisch<sup>1</sup>  | Arne S. Schaefer<sup>1</sup> 

<sup>1</sup>Department of Periodontology, Oral Medicine and Oral Surgery, Institute for Dental and Craniofacial Sciences, Berlin Institute of Health, Charité—University Medicine Berlin, Corporate Member of Freie Universität Berlin, Humboldt-Universität zu Berlin, Berlin, Germany

<sup>2</sup>Institute of Medical Informatics and Statistics, Kiel University, University Hospital Schleswig-Holstein, Kiel, Germany

<sup>3</sup>Core Unit Bioinformatics, Berlin Institute of Health, Berlin, Germany

## Correspondence

Arne S. Schaefer, Department of Periodontology, Oral Medicine and Oral Surgery, Institute for Dental and Craniofacial Sciences, Berlin Institute of Health, Charité—University Medicine Berlin, Corporate Member of Freie Universität Berlin, Humboldt-Universität zu Berlin, Berlin, Germany.  
Email: [arne.schaefer@charite.de](mailto:arne.schaefer@charite.de)

## Funding information

German Research Foundation, Grant/Award Number: SCHA1582 5-1; Christian-Albrecht University of Kiel, Grant/Award Number: K 126 202

[Correction added on 25 August 2022, after first online publication: The funding information, the 3rd author's name and contribution was corrected in this version.]

## Abstract

**Aim:** The basis of phenotypic variation of periodontitis is genetic variability. Disease relevant effects of individual risk alleles are considered to result from genetic interactions. We investigated gene  $\times$  gene ( $G \times G$ ) interactions of suggestive periodontitis susceptibility alleles.

**Materials and Methods:** We used the case-only design and investigated single-nucleotide polymorphism (SNPs) that showed associations in our recent genome-wide association study (GWAS) and GWAS meta-analysis with  $p < 5 \times 10^{-6}$ . CRISPR-dCas9 gene activation followed by RNA-sequencing and gene-set enrichment analyses elucidated differentially expressed genes and gene networks. With the databases of SNPInspector and Transfac professional, luciferase reporter gene assays and antibody electrophoretic mobility shift experiments, we analysed allele-specific effects on transcription factor binding.

**Results:** SNPs at the genes sialic acid binding Ig-like lectin 5 (*SIGLEC5*) and plasminogen (*PLG*) showed  $G \times G$  interactions with rs1122900 at the long non-coding RNA (lncRNA) *CTD-2353F22*. Associated chromatin cis-activated *CTD-2353F22.1* 6.5-fold ( $p = .003$ ), indicating *CTD-2353F22.1* as target gene of this interaction. *CTD-2353F22.1* regulated *GADD45A* ( $p_{\text{adj}} < 4.9 \times 10^{-11}$ ,  $\log_2$  fold change (FC) =  $-0.55$ ), *THBS1*, *SERPINE1* and *Tissue Factor F3* ( $p_{\text{adj}} < 5 \times 10^{-7}$ ,  $\log_2$  FC  $\geq -0.35$ ) and the gene set “angiogenesis” (area under the curve = 0.71,  $p_{\text{adj}} = 8.2 \times 10^{-5}$ ). rs1122900 effect C-allele decreased reporter gene activity (5.5-fold,  $p = .0003$ ) and PRDM14 binding (76%).

Ricarda Müller and Sandra Freitag-Wolf contributed equally.

This is an open access article under the terms of the [Creative Commons Attribution-NonCommercial](https://creativecommons.org/licenses/by-nc/4.0/) License, which permits use, distribution and reproduction in any medium, provided the original work is properly cited and is not used for commercial purposes.

© 2022 The Authors. *Journal of Clinical Periodontology* published by John Wiley & Sons Ltd.

**Conclusions:** CTD-2353F22.1 mediates interaction of *SIGLEC5* and *PLG*, together with genes that function in periodontal wound healing.

#### KEYWORDS

angiogenesis, case-only design, gene–gene interaction, lncRNA, periodontitis

#### Clinical Relevance

*Scientific rationale for study:* Disease relevant effects of genetic risk factors are considered to result from interacting susceptibility alleles.

*Principal findings:* We found that risk alleles of *SIGLEC5* and *PLG* genetically interact with the long non-coding RNA CTD-2353F22.1, which regulates genes with a role in wound healing and angiogenesis.

*Practical implications:* Our results emphasize the important role of wound healing and vascularization in the pathogenesis of periodontitis. These mechanisms may be particularly affected in patients with a genetic susceptibility to periodontitis.

## 1 | INTRODUCTION

Periodontitis is an oral inflammatory disease with a wide range of manifestations that differ in severity, progression of tissue destruction and age of disease onset. The basis of the phenotypic variation is genetic variability between different individuals (Timpson et al., 2018). Genetic variants mostly are single-nucleotide polymorphisms (SNPs) (Genomes Project et al., 2015) and the number of functional SNPs, their specific biological consequences, magnitude of effects and interactions with each other and with environmental factors form the genetic architecture that influences and shapes disease manifestation (Boyle et al., 2017; Wray et al., 2018). For periodontitis, several genome-wide association study (GWAS) were performed to identify specific genetic risk variants. However, the proportion of heritability explained by these associations is small. This is consistent with other complex diseases and implies a genetic architecture of many risk loci with moderate effect sizes (Visscher et al., 2017). It is considered that a disease phenotype that impacts only a small fraction of the population and has a genetic architecture of common risk loci with low or moderate effects, such as early-onset periodontitis, is best explained by a non-linear relationship between the disease and the burden of risk alleles (Wray et al., 2018). In this view, the consequences of the effects of the risk alleles are non-additive but are caused by interacting genetic effects. This implies that many individuals in the population carry risk variants, but specific combinations have non-additive deleterious consequences that strongly contribute to the individual disease risk (Wray et al., 2018). The knowledge of these gene  $\times$  gene (G $\times$ G) interactions and their biological consequences has strong potential to contribute to a better understanding of the particular causation of the disease and may improve disease treatment or prevention.

Early-onset, severe phenotypes are considered to have a high heritability. We recently performed a GWAS with generalized stage III grade C periodontitis with an age of first diagnosis  $\leq 35$  years to better understand the biology of this disease (Munz et al., 2017). In that study, we identified three loci with suggestive associations

( $p < 5 \times 10^{-6}$ ) and two loci with genome-wide significance ( $p < 5 \times 10^{-8}$ ), which were the inhibitory immune receptor gene sialic acid binding Ig-like lectin 5 (*SIGLEC5*) and the antimicrobial peptides alpha defensin gene *DEFA1A3*. The association with *SIGLEC5* was subsequently validated by a GWAS meta-analysis of periodontitis (Shungin et al., 2019). Additionally, in a meta-analysis of generalized stage III grade C periodontitis and more moderate forms of periodontitis ( $\leq 60$  years of first diagnosis), comprising 5095 cases and 9908 controls, we found two novel loci that were associated with periodontitis at genome-wide significance level and four loci that showed suggestive associations (Munz et al., 2019).

In the current study, we hypothesized that G $\times$ G interactions exist between these associations. The objective of this study was to identify putative interactions of SNPs that showed associations with  $p < 5 \times 10^{-5}$  in our GWAS and GWAS meta-analysis. A workflow illustrating the experimental approach and the main results is shown in Figure S1.

## 2 | MATERIALS AND METHODS

### 2.1 | G $\times$ G interaction analysis

For the statistical analysis of G $\times$ G interactions, we used GWAS genotypes of 896 North-West European periodontitis cases, with 30% bone loss at  $>2$  teeth diagnosed  $\leq 35$  years (Munz et al., 2017). This diagnosis indicated severe, rapid disease progression corresponding to stage III grade C periodontitis (Caton et al., 2018). We used the case-only design to analyse G $\times$ G interactions. This study design provides a considerable gain in power over classical case–control analyses and has been applied to identify G $\times$ G and G–environment interactions (Piegorisch et al., 1994; Freitag-Wolf et al., 2019, 2021; Aleknyyte-Resch et al., 2020). We calculated the statistical power to detect G  $\times$  G with the case-only design post hoc using Quanto software (Gauderman, 2002). We fixed effects parameters as follows: disease prevalence = 0.1%, MAF according to the associated SNPs at *SIGLEC5*

(MAF = 0.2) and PLG (MAF = 0.4), and odds ratio (OR) = 1.75. With these parameters, our case sample had a power of 0.94. With the case-control design (considered a 1:1 case-control ratio), the power was 0.75. The statistical model is described in detail in Appendix. Additionally, we validated the assumed statistical independence of genotypes in our GWAS controls ( $N = 7104$ , described in (Munz et al., 2017)) using the Wald test as described in detail in Supplementary Methods. For further analyses, we included only SNP pairs with  $p > .1$  in the controls, which confirmed that G1 and G2 are independent in the population. A significant result of the same test in the cases indicates interactions between G1 and G2.

To limit the family-wise error rate of the association tests to 5%, Bonferroni correction was applied, dividing the conventional  $p$  value threshold of .05 by the number of SNP pairs considered to obtain a test-wise threshold. Starting with 10 SNP associations selected from the GWAS and GWAS meta-analysis, we compared a total of 45 SNP interactions. All statistical analyses were performed with PLINK 21 and R (v. 3.5.0).

## 2.2 | Bioinformatical investigations of expressed quantitative trait loci, linkage disequilibrium and transcription factor binding sites

Methods used for expressed quantitative trait loci (eQTL), linkage disequilibrium (LD) and transcription factor binding sites (TFBS) analyses are explained in Appendix.

## 2.3 | 5'- and 3'-RACE-PCR and qRT-PCR

To obtain the full length sequences of *CTD-2353F22.1* transcripts expressed in the B cell line GM12878 and in primary CD19+ primary B cells (RNA purchased from Miltenyi Biotec, Germany), we performed RACE-PCR and quantitative Real-Time PCR (qRT-PCR) as described in Appendix.

## 2.4 | CRISPR-dCas9 activation, RNA-Sequencing, luciferase reporter gene assays and electrophoretic mobility shift assay

These methods were performed as recently described (Chopra et al., 2021) and we give all experimental details in Appendix.

# 3 | RESULTS

## 3.1 | SNPs at *SIGLEC5* and *PLG* showed gene $\times$ gene interaction with rs122900 at *lncRNA CTD-2353F22.1*

We performed a G $\times$ G interaction analysis with SNPs that showed association with periodontitis at  $p < 5 \times 10^{-6}$  in our previous GWAS

(Munz et al., 2017) and GWAS meta-analysis (Munz et al., 2019). For these SNPs, we found G $\times$ G interactions with  $p < .01$  between rs122900 at the *lncRNA CTD-2353F22* and rs4284742 (*SIGLEC5*) and rs1247559 (*PLG*), with  $p = .0057$  and  $p = .0092$ , respectively (Table 1). The G $\times$ G interaction of these SNPs suggested an interaction OR of 1.6. This indicates that the interaction of the risk alleles gives an additional risk that is above the additive effect of the individual risk alleles.

## 3.2 | eQTLs and CRISPRa indicated *CTD-2353F22* as the target gene of the rs122900-association

eQTL data showed that *SIGLEC5* was the target gene of the association with periodontitis (rs4284742, whole blood:  $p = 7.7 \times 10^{-14}$ ) (Westra et al., 2013). A study that investigated SNP associations with PLG levels in blood plasma identified the rare rs2565722-T allele, which is correlated with the G $\times$ G interacting SNP rs1247559 at PLG ( $r^2 = 0.73$ ), to be associated with 0.42 unit increase of protein plasminogen (Suhre et al., 2017). This also implied *PLG* as target gene of the association.

For SNP rs122900, eQTL effect was observed on *CTD-2353F22.1* (whole blood:  $p = 6 \times 10^{-15}$ ) (Figure 1) (eGTEx Project, 2017). This indicates *CTD-2353F22* as the target gene of the association. Using CRISPRa, we tested whether the chromatin elements at rs122900 were able to cis-activate *CTD-2353F22.1* expression, to validate *CTD-2353F22.1* as a target gene. We transfected six sgRNAs that covered 2600 basepairs (bp) of the chromatin at rs122900. One sgRNA (chr19:36690687–36690704, hg19), located 1.506 nucleotides downstream of rs122900 (chr5:36689181, hg19), induced *CTD-2353F22.1* expression 2.7-fold ( $p = .003$ ; Figure 2). Expression of the neighbouring protein-coding gene solute carrier family 1 member 3 (*SLC1A3*) *SLC1A3* was not increased by CRISPRa.

We previously reported a second haplotype block at *CTD-2353F22* that showed association with stage III grade C periodontitis (Munz et al., 2017). This block is correlated with rs122900 ( $r^2 = 0.74$ ) and tagged by rs6887423, which is in strong LD ( $r^2 > 0.8$ ) with three other SNPs (Figure 1). eQTL data indicated additive activating regulatory effects in carriers of the rs6887423 C-allele on *CTD-2353F22* expression in blood ( $p = 2.6 \times 10^{-26}$ ), but not on other genes. We performed CRISPRa with three gRNAs that covered 167 bp of the chromatin at rs6887423. A gRNA (chr19:36696573–36696591) that located 72 bp downstream rs6887423 induced *CTD-2353F22.1* expression 6.5-fold ( $p = .003$ ) compared with the scrambled gRNA (Figure 2) but not *SLC1A3*. This indicated that *CTD-2353F22* is the target gene of the association with periodontitis.

## 3.3 | *CTD-235322* is primarily expressed as an intergenic *lncRNA*

*CTD-2353F22* is expressed at the highest levels in mast cells (39.5 counts per million [CPM]), B cells (22.9 CPM) and dendritic cells (17.2

**TABLE 1** G×G interaction analysis shows the interaction of single-nucleotide polymorphisms (SNPs) at *SIGLEC5* and *PLG* with rs1122900 at *CTD-2353F22.1*

	Gene	SNP	Effect size in GWAS (risk allele)	p Value (GWAS association)	G×G interaction partner	SNP	OR (risk allele × risk allele)	p <sup>a</sup>
GWAS <sup>b</sup>	<i>SIGLEC5</i>	rs4284742	1.33 (G)	$1.3 \times 10^{-8}$	<i>CTD-2353F22</i>	rs1122900	1.604 [1.586–1.622]	.0057
	<i>DEFA1A3</i>	rs2738058		$6.8 \times 10^{-10}$	None			
	<i>CTD-2353F22</i>	rs1122900	1.26 (A)	$8.0 \times 10^{-7}$	<i>SIGLEC5</i>		n.s.	
	<i>OSTCP2</i>	rs4970469		$1.2 \times 10^{-6}$	None			
	<i>FCER1G</i>	rs2070901		$4.4 \times 10^{-6}$	None			
GWAS meta-analysis <sup>c</sup>	<i>ATP6V1C1</i>	rs16870060		$3.7 \times 10^{-9}$	None			
	<i>LOC107984137</i>	rs729876		$9.77 \times 10^{-9}$	None			
	<i>PLG</i>	rs1247559	1.21 (T)	$2.25 \times 10^{-5}$	<i>CTD-2353F22</i>	rs1122900	1.601 [1.582–1.620]	.0092
	<i>MCM3AP</i>	Rs9982623		$5.7 \times 10^{-7}$	None			
	<i>MAPK6PS2</i>	Rs9984417		$3.2 \times 10^{-6}$	None			

Abbreviation: OR, odds ratio.

<sup>a</sup>Two-sided Wald test in the case-only design.<sup>b</sup>Munz et al. (2017).<sup>c</sup>Munz et al. (2019).

CPM), with enrichment of 16.8-fold ( $p = 4.7 \times 10^{-7}$ ), 9.2-fold ( $p = 1.3 \times 10^{-7}$ ) and 6.6-fold ( $p = 1.9 \times 10^{-5}$ ), respectively, compared with other cells (Fantom 5 data) (Lizio et al., 2015; Abugessaisa et al., 2021). *CTD-2353F22* is expressed in different transcripts (Figure 1). These are an antisense lncRNA *ENST00000510740* (spliced RNA 478 bp), which overlaps with the sequence of *SLC1A3*, and two intergenic transcripts that terminate 12 kb downstream *SLC1A3* (*ENST00000512329*, 1924 bp; *ENST00000508745*, 589 bp). We validated the expression of *CTD-2353F22* antisense and intergenic transcripts by RACE-PCR in the B cell line GM12878 and in primary CD19+ primary B cells. Sequencing of the 5'- and 3'-RACE products validated the expression of the two intergenic transcripts and of the antisense transcript. Notably, qRT-PCR showed a 4.0-fold (GM12878) and 4.6-fold (CD19+) higher expression of the intergenic transcripts compared with the antisense transcript. RACE-PCR detected no expression of the truncated 2 exon transcript or other transcript isoforms.

### 3.4 | Overexpression of *CTD-2353F22* downregulates genes of the coagulation cascade and activates genetic pathways involved in response to wounding and re-vascularization

Intergenic lncRNAs often function in trans-acting mode to target distant gene loci, while antisense lncRNAs, which are transcribed from the opposite strand of a protein-coding gene, commonly downregulate their neighbouring antisense gene (Chu et al., 2011). Having shown that *CTD-2353F22* is the target gene of the association with rs1122900 and is largely expressed as an intergenic

RNA, we were interested in identifying genes and pathways that respond to *CTD-2353F22* expression. We targeted sgRNAs to the promoter of *CTD-2353F22* for using CRISPRa to induce *CTD-2353F22* expression in the native chromatin context. We observed that the transfection efficiency of CRISPRa was considerably higher in HeLa cells compared with B cells, with a transfection efficiency of 70%–80% and 20%–25%, respectively. Because higher transfection efficiency results in a higher number of transfected cells, and thus in reduced confounding by untransfected cells, we used CRISPRs in HeLa cells. First, we tested whether the expression ratio of the *CTD-2353F22* isoforms was identical to B cells and performed qRT-PCR from cDNA of CRISPR activated HeLa cells with our RACE-PCR primers. Expression of intergenic transcripts *ENST00000512329* and *ENST00000508745* strongly increased with FC = 34 ( $p = .002$ ) and FC = 37 ( $p = .0004$ ), respectively. In agreement with our RACE-PCR data in the B cell line GM12878 and in CD19+ primary B cells, antisense transcript *ENST00000510740* showed the lowest expression with FC = 5.1 ( $p = .01$ ; Figure 3). This indicated that CRISPRa in HeLa induced no artificial transcript bias.

Next, we performed RNA-sequencing of total RNA from CRISPR activated HeLa cells compared with HeLa cells transfected with scrambled sgRNA as controls. *CTD-235322.1* was the most upregulated gene with a 49× fold change (FC  $\log_2 = 5.6$ ;  $p_{\text{adj}} < 7.5 \times 10^{-35}$ ). No other gene was upregulated with FC  $\geq 1.3$  (Table 2), indicating that *CTD-235322* is not an activating lncRNA. In contrast, several genes showed strong downregulation. Of these, *GADD45A* (Growth Arrest And DNA Damage Inducible Alpha) was most significantly downregulated (adjusted  $p$ -value  $p_{\text{adj}} < 4.9 \times 10^{-11}$ ,  $\log_2$  FC = −0.55). Notably, three genes of the coagulation cascade were among the top five most

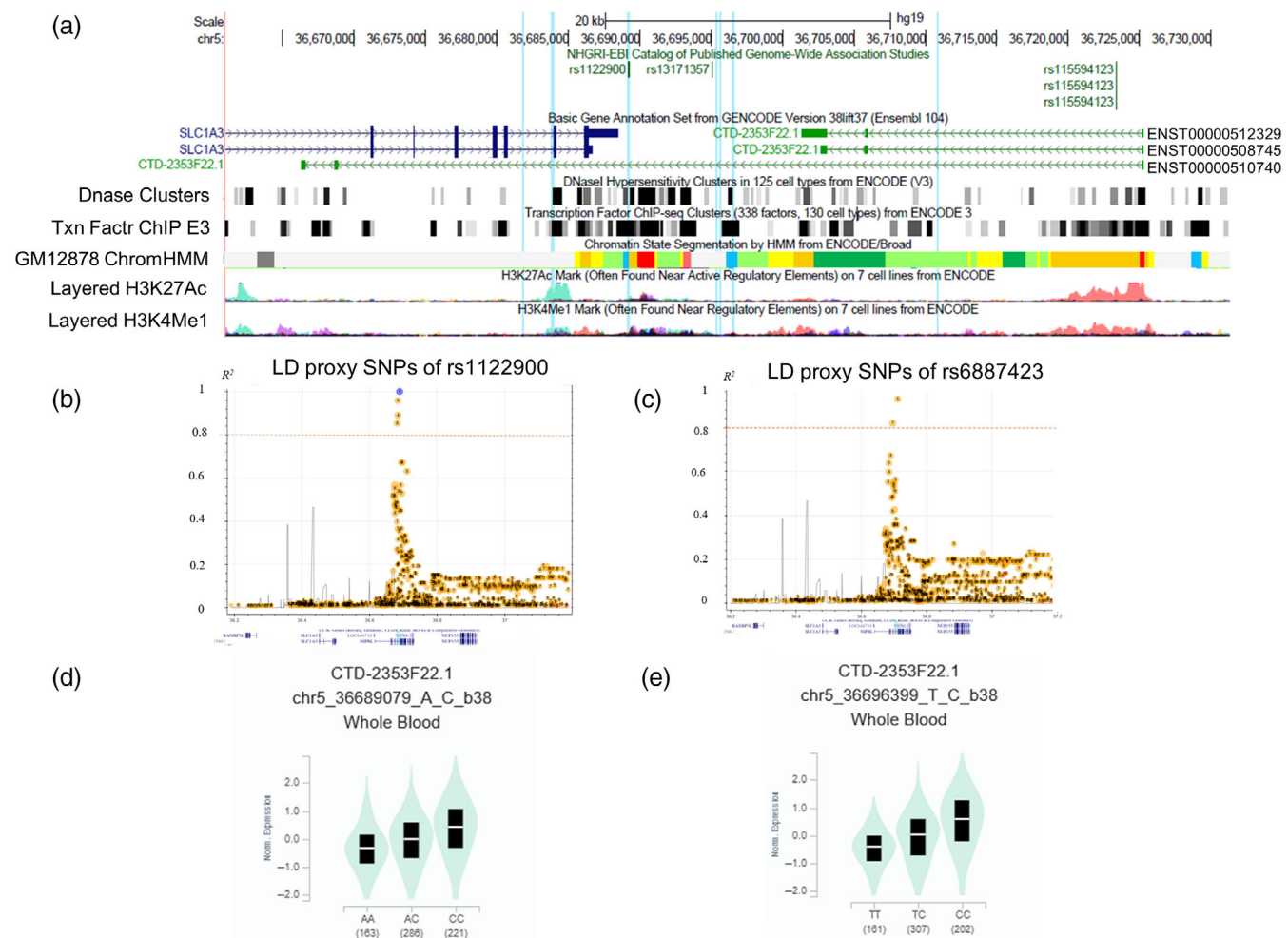


**FIGURE 1** Chromosomal positions of the gene *CTD-2353F22.1* and periodontitis-associated single-nucleotide polymorphisms (SNPs). (a) *CTD-2353F22.1* is expressed in one antisense transcript and two intergenic isoforms. The eight periodontitis-associated SNPs are marked with light blue vertical lines. SNP order from left to right: rs6862950, rs56038114, rs56039629, rs1122900, rs17585785, rs56066032, rs6887423 and rs56162483. From top: The first panel shows the chromosomal hg19 positions and the exon-intron structure of the genes. *CTD-2353F22.1* is transcribed in reverse orientation to *SLC1A3*. The second panel shows the ENCODE-derived DNase I hypersensitive sites from 125 cell types. These accessible chromatin zones are functionally related to transcriptional activity. The next panel presents the binding regions that were determined for 338 transcription factors (TFs) by chromatin immunoprecipitation sequencing (ChIP-seq) experiments of ENCODE. This panel does not show the exact transcription factor binding site but indicates TF binding was found at these chromatin regions. The subsequent panel displays chromatin state segmentation for the human cell line GM12878, generated with ChIP-seq data for nine TFs functionally related to transcriptional activity as input. The states are coloured to highlight predicted functional elements (orange = strong enhancer, yellow = weak enhancer, green = weak transcribed, blue = insulator, red = active promoter, purple = poised promoter). The bottom panel shows ENCODE-derived H3K4me1 and H3K27ac methylation marks from seven cell lines that are often associated with the higher activation of transcription and are defined as active enhancer marks. The figure was generated using UCSC Genome Browser. (b, c) Three SNPs are correlated with rs1122900 and with rs6887423 at  $r^2 > 0.8$  (dashed horizontal line; figures generated with LDproxy Tool with CEU and GBR samples). (d, e) The common C alleles of rs1122900 and rs6887423 increase *CTD-2353F22.1* expression. eQTL violin plot with expression data in whole blood (GTEx Analysis Release V8 [dbGaP Accession phs000424.v8.p2]). Note that in European populations the common alleles of these SNPs are not ancestral in African populations (rs1122900, EU: A = 0.42, C = 0.58, AFR: A = 0.88, C = 0.12; rs6887423, EU: T = 0.45, C = 0.55, AFR: T = 50, C = 0.50).

significant downregulated genes ( $p_{\text{adj}} < 5 \times 10^{-7}$ ,  $\log_2 \text{FC} \geq -0.35$ ). These genes were *THBS1* (Thrombospondin 1), *SERPINE1* (Serpin Family E Member 1) and *Tissue Factor F3* (Coagulation Factor III).

GO term enrichment analysis showed highest enrichment for the terms “Response to Wounding”, “Blood Vessel Morphogenesis”, followed by “angiogenesis” and “inflammatory response” (Figure 3b).

Gene-set enrichment analysis using a second-generation algorithm showed the highest effect sizes for the gene set “angiogenesis” (area under the curve [AUC] = 0.71,  $p_{\text{adj}} = 8.2 \times 10^{-5}$ ), “E2F Targets” (AUC = 0.67,  $p_{\text{adj}} = 1.5 \times 10^{-13}$ ), “MYC Targets V2” (AUC = 0.65,  $p_{\text{adj}} = 1.1 \times 10^{-4}$ ) and “TNF alpha signalling via NFkB” (AUC = 0.63,  $p_{\text{adj}} = 1.0 \times 10^{-17}$ ; Figure 4).



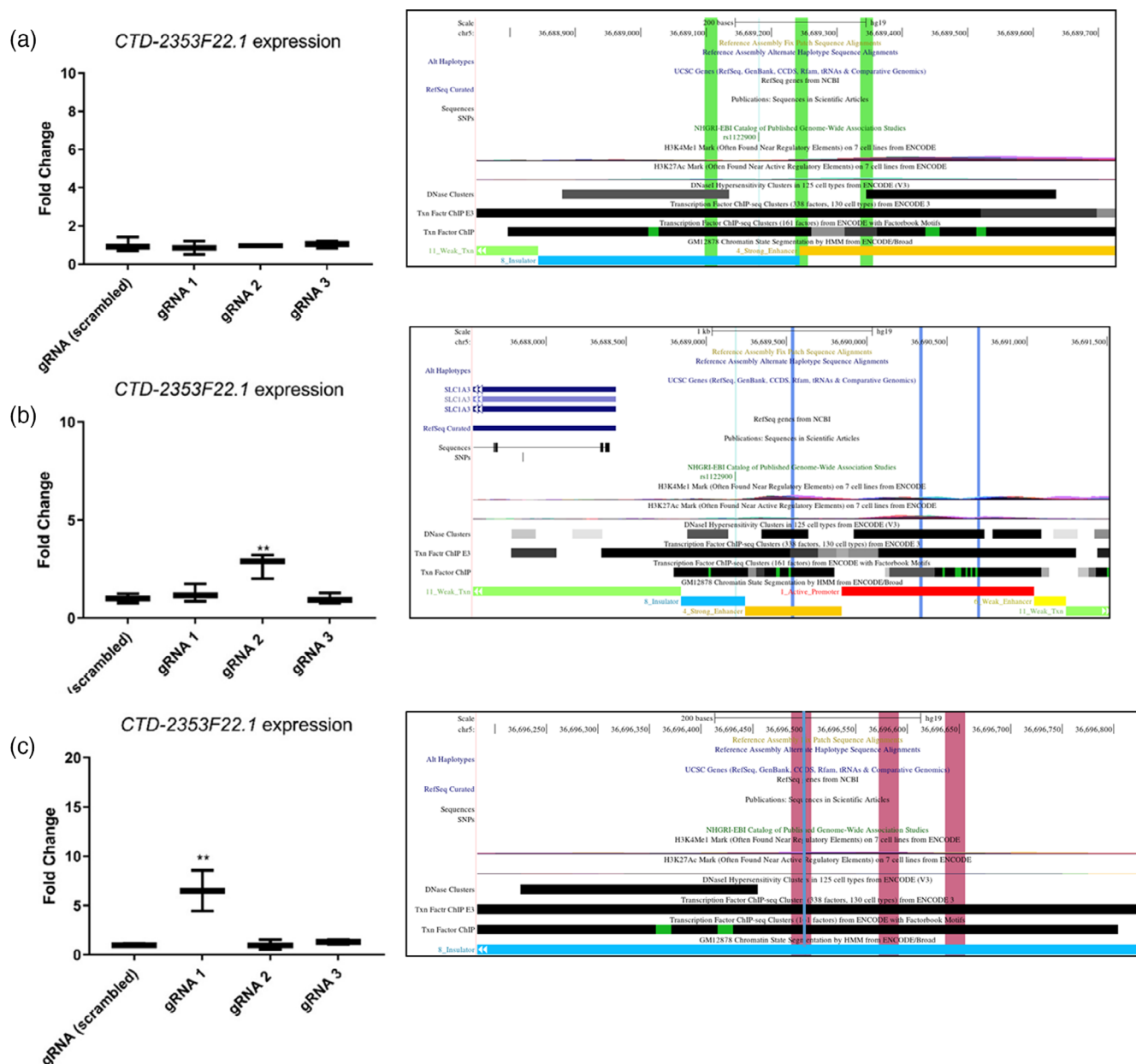


**FIGURE 2** CRISPRa at rs1122900 and rs6887423 increases CTD-2353F22.1 expression. (a) CRISPRa with gRNAs that aligned directly at the genomic region at rs1122900 showed no effect on CTD-2353F22.1 expression. (b) CRISPRa with gRNAs that aligned in a distance of 2100–2600 bp downstream of rs1122900 activated CTD-2353F22.1 expression 2.7-fold ( $p = .003$ ). (c) CRISPRa with a gRNA that aligned directly at rs6887423 with gRNA 1 induced CTD-2353F22.1 expression 6.5-fold ( $p = .003$ ). The coloured bold vertical lines in the right panels show the chromosomal positions of the gRNAs, the light blue thin vertical lines show the positions of rs1122900 (right upper and middle panel) and rs6887423 (right bottom panel). \* $p < .05$ , \*\* $p < .005$

### 3.5 | rs1122900-C is a functional allele that impairs expression and PRDM14 binding

rs1122900 and rs6887423 were located on correlated haplotype blocks ( $r^2 = 0.67$ ). Each of these SNPs was in strong LD ( $r^2 > 0.8$ ) with three further SNPs (Figure 1). We bioinformatically investigated whether the different alleles of these eight SNPs changed predicted TFBSs. At rs1122900, we found a predicted TFBS for the TF PRDM14 (PWM similarity score = 89%, Figure 5). At rs6887423, we

found a TFBS for AHR (PWM similarity score = 100%) and at rs56038114, we found a predicted TFBS for GATA1 (PWM similarity score = 96%, Figure S2). None of the databases predicted allele-specific TFBS at the other five SNPs. The three disease-associated SNPs with predicted TFBS were located at DNase I hypersensitivity clusters (determined by ENCODE; Figure 1), indicating chromatin accessibility.

To test whether the DNA sequences at rs1122900, rs6887423 and rs56038114 had allele-specific effects on gene

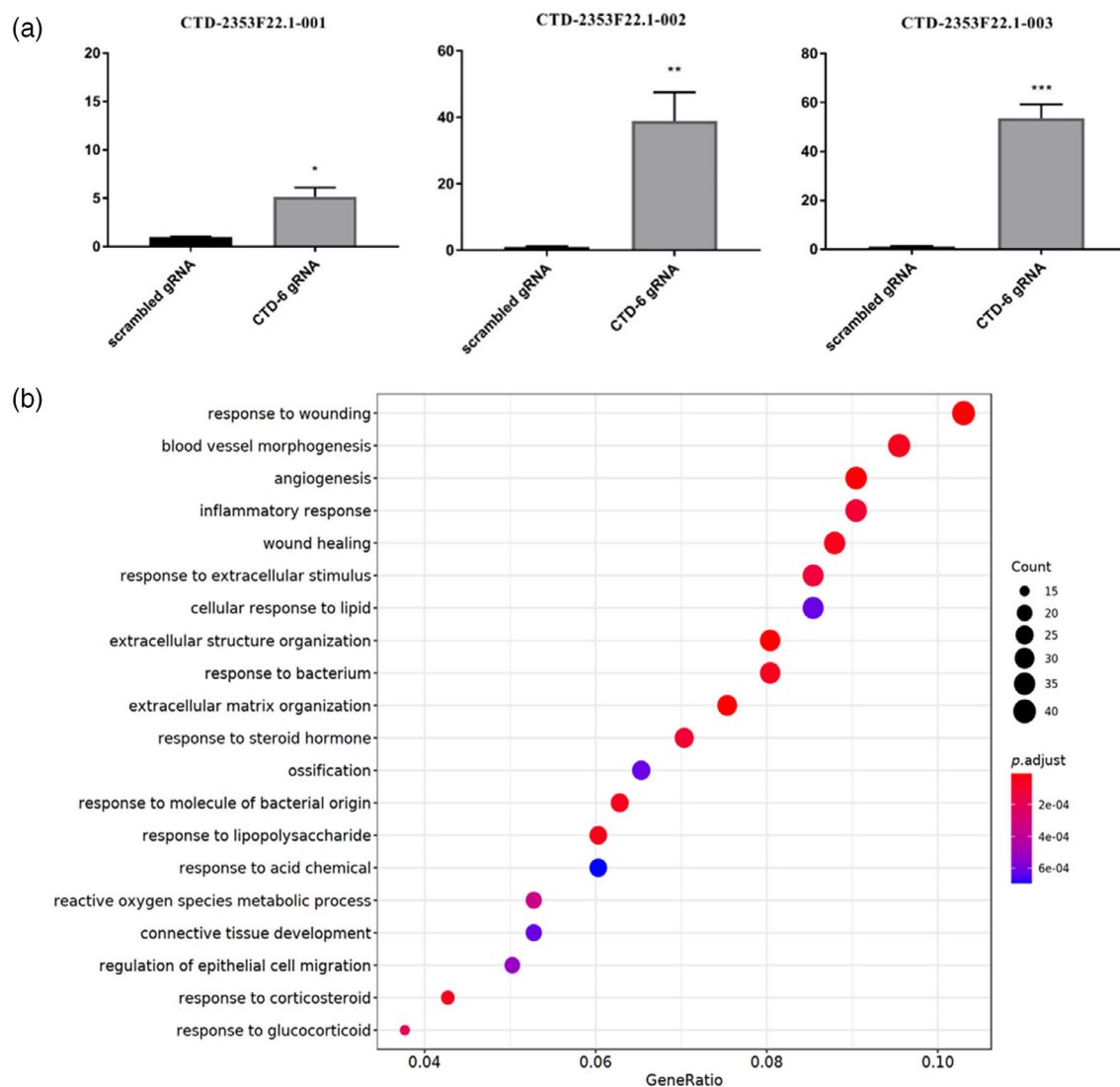


**FIGURE 3** CTD-2353F22.1 has a role in the regulation of wound healing and vascularization. (a) CRISPR-dCas9 activation of the CTD-2353F22.1 promoter in HeLa cells upregulated the antisense transcript ENST00000510740.1 (–001) 5.1-fold ( $p = .01$ ). In contrast, the intergenic transcripts ENST00000512329.1 and ENST00000508745.1 were upregulated 34-fold ( $p = .002$ ) and 37-fold ( $p = .0004$ ), respectively. This expression ratio was concordant to that found in the B cell lymphocyte cell line GM12878 and primary CD19+ B cells by RACE-PCR, indicating that CRISPRa in HeLa cells corresponds with B cell expression (see text). (b) Dot plot of GO enrichment analysis shows the highest enrichment for the terms “Response to Wounding” and “Blood Vessel Morphogenesis”, followed by “Angiogenesis” and “Inflammatory response”. Dots represent term enrichment (red = high enrichment, blue = low enrichment; dot sizes represent the counts of each row of the GO category).

activity, we cloned  $\leq 147$  bp spanning each SNP allele upstream of the luciferase reporter gene promoter and transfected the reporter plasmids into HeLa cells. The rs1122900-A reporter gene increased luciferase activity 5.5-fold compared with the empty plasmid ( $p = .0003$ ), whereas the rs1122900-C reporter gene showed no increase in luciferase activity (Figure 5). This indicated allele-specific enhancer function of the DNA sequence at rs1122900. In contrast, the DNA sequence at rs6887423-sequence showed no effect on luciferase activity. Likewise, the sequence containing the common allele of rs56038114 did not affect the luciferase gene expression, although the sequencing with the rare C-allele, which was predicted to reduce GATA1 binding affinity, increased

the expression 2.2-fold ( $p = .01$ ). After correcting for six independent measurements, we considered this effect not significant. These data implied that rs6887423 and rs56038114 were not functional SNPs that are causative for the periodontitis association.

Next, we tested if PRDM14 binds at the predicted TFBS at rs1122900. We performed a PRDM14-antibody electrophoretic mobility shift assay (EMSA) with rs1122900 allele-specific oligonucleotide probes and nuclear protein extract from the B cell line Raji. Binding of PRDM14-antibody to allele-specific probes with the effect C-allele abrogated antibody binding compared with probes with the A-allele by 76% (Figure 5).

**TABLE 2** Up- and downregulated genes ( $p_{\text{adj}} < 5 \times 10^{-6}$ ) after CRISPRa of CTD-2353F22.1 in HeLa cells

Gene	Description	Fold change (log <sub>2</sub> )	p Value	$p_{\text{adj}}$ Value
Upregulated genes				
CTD-2353F22.1	Uncharacterized lncRNA	5.61	6.4E-39	7.5E-35
LPL	Lipoprotein lipase	0.34	1.1E-14	4.9E-11
CPS1	Carbamoyl-phosphate synthase 1	0.31	7.9E-14	2.3E-10
RNF182	Ring finger protein 182	0.29	6.2E-10	8.1E-07
ASS1	Argininosuccinate synthase 1	0.38	7.7E-10	9.0E-07
ATP9A	ATPase phospholipid transporting 9A	0.36	4.5E-09	4.4E-06
CBX5	Chromobox 5	0.29	4.9E-09	4.4E-06
Downregulated genes				
GADD45A	Growth arrest and DNA damage inducible alpha	-0.55	1.25E-14	4.89E-11
THBS1	Thrombospondin 1	-0.35	4.98E-13	1.17E-09
SERPINE1	Serpin family E member 1	-0.46	2.45E-12	4.78E-09
F3	Coagulation factor III, tissue factor	-0.50	1.65E-10	2.76E-07
FOSL1	FOS Like 1, AP-1 transcription factor subunit	-0.64	2.82E-10	4.12E-07
NBPF19	Neuroblastoma breakpoint family member 19	-0.63	1.22E-09	1.30E-06

## 4 | DISCUSSION

In this study, we searched for G×G interactions of common risk variants identified in our previous GWAS (Munz et al., 2017) and GWAS meta-analysis (Munz et al., 2019) that were associated with  $p < 5 \times 10^{-6}$ . We identified G×G interaction of variants at *SIGLEC5* and *PLG* with a variant at the intergenic lncRNA *CTD-2353F22.1*. Mast cells, B cells and dendritic cells primarily express *CTD-2353F22.1*, implying a role of this lncRNA in immune regulation. Intergenic lncRNAs often function in trans-acting mode to target distant gene loci (Chu et al., 2011). Accordingly, we observed that following upregulation of *CTD-2353F22.1*, distant genes were downregulated but not the neighbouring gene.

The gene that showed most significant downregulation was *GAD45A*, which is activated following stressful growth arrest conditions and DNA damage and inhibits entry of cells into S phase (Takekawa & Saito, 1998; Tran et al., 2002). The next three most significantly downregulated genes were *THBS1*, *SERPINE1* and *Coagulation Factor F3*, which have roles in coagulation and wound healing. Thrombospondin-1 is a potent inhibitor of angiogenesis (Streit et al., 2000) in response to vascular injury and cytokines (reviewed in Simantov & Silverstein, 2003). *SERPINE1* encodes the plasminogen activator inhibitor 1 (PAI), which is involved in fibrinolysis and blood clot degradation (Lee et al., 1993; Fay et al., 1997; Jankun et al., 2007), regulation of cell adhesion (Planus et al., 1997) and stimulation of keratinocyte migration during cutaneous injury repair (Providence et al., 2008). The expression of *coagulation factor F3* by adventitial fibroblasts and vascular smooth muscle cells provides a haemostatic barrier that activates coagulation when vascular integrity is disrupted (Drake et al., 1989). Coagulation with robust thrombin generation leading to fibrin formation is necessary for wound healing. Likewise, in the wound bed, expression of proteolytic enzymes such

as *PLG* (Silva et al., 2021) and their inhibitors like *SERPINE1* (PAI-1) provide a mechanism for fine control of proteolysis to facilitate matrix restructuring during wound healing (Simone et al., 2014).

Corresponding to these top downregulated genes, the gene-set enrichment analysis showed the highest effect sizes for the gene sets “angiogenesis” and wound healing. During wound healing of tissue injuries, angiogenic capillary sprouts invade the wound clot and organize into a microvascular network throughout the granulation tissue (reviewed in Tonnesen et al., 2000). Taken together, our data suggest that lncRNA *CTD-2353F22.1* has a putative role in the regulation of these processes. Furthermore, the identified G×G interaction of lncRNA *CTD-2353F22.1* with *PLG* and *SIGLEC5* implies that these genes are functionally linked.

Most wounds at tissue–environment interfaces will cause leakage of blood from damaged vessels with subsequent formation of a blood clot that consists of platelets embedded in a mesh of cross-linked fibrin fibres. Clot formation serves as a temporary shield protecting the wounded tissue to prevent bacterial spread and provides a provisional matrix over and through which cells can migrate during the repair process (Opneja et al., 2019). However, tissue regeneration in response to wounding requires subsequent resolving of fibrin clots. For the protease plasmin, the active form of plasminogen, the principal physiological target is fibrin. Likewise, defective wound healing and periodontitis characterize *PLG* deficiency (Silva et al., 2021). Moreover, for wound healing in an aseptic commensal environment like the oral cavity, discrimination of tissue injuries from pathogenic infections is required. Here, the innate immune system uses danger (DAMPs)- and pathogen-associated molecular patterns that originate from wounding or injuries by pathogenic infection, respectively, and are recognized through Toll-like receptors (TLR). Sialoside-based pattern recognition by *SIGLEC* receptors selectively suppresses the TLR-response to DAMPs, suggesting a mechanism that allows wound



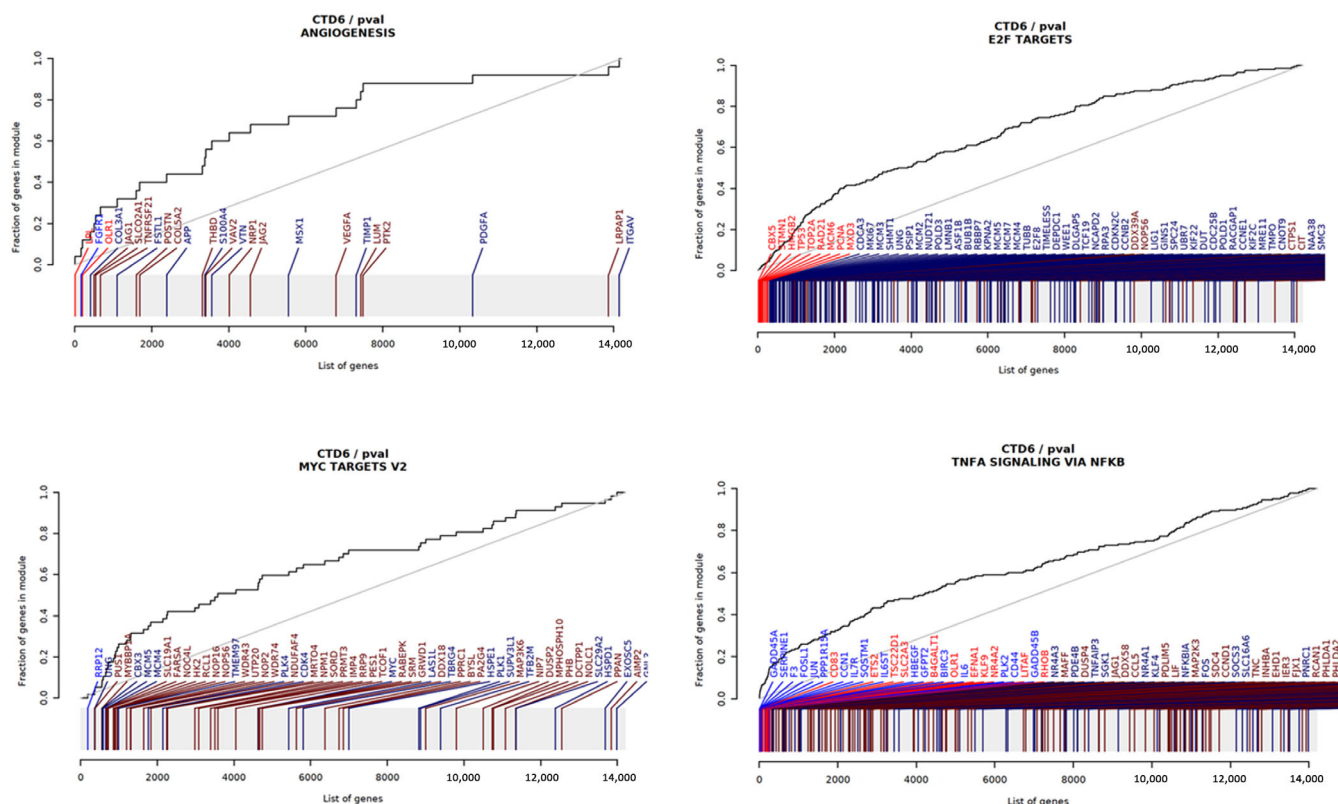


**FIGURE 4** Gene-set enrichment analysis of CRISPRa induced *CTD-2353F22.1* expression in HeLa cells. Shown are evidence plots (receiver-operator characteristic curves) for the top four gene sets. The highest effect sizes of the *CTD-2353F22.1* CRISPRa cells compared with scrambled sgRNA were found for the gene sets “Angiogenesis” (upper left) with an area under curve (AUC) = 0.71 ( $p$ -value  $p_{adj} = 8.2 \times 10^{-5}$ ), “E2F Targets” (upper right; AUC = 0.67,  $p_{adj} = 1.5 \times 10^{-13}$ ), “MYC Targets V2” (lower left; AUC = 0.65,  $p_{adj} = 1.1 \times 10^{-4}$ ) and “TNF alpha signalling via NFKB” (lower right; AUC = 0.63,  $p_{adj} = 1.0 \times 10^{-17}$ ). The grey rug plot underneath each curve corresponds to genes sorted by  $p$ -value, with the genes belonging to the corresponding gene sets highlighted in red (upregulated genes) or blue (downregulated genes). Bright red or bright blue indicates that the genes were significantly regulated. The AUC corresponds to the effect size of the enrichment, with .5 being no enrichment and 1.0 being maximal possible enrichment.

healing in the presence of commensal microorganisms (Chen et al., 2009). The observed  $G \times G$  interaction may indicate a physiological link between fibrinolysis and innate immune suppression during commensal aseptic wound healing. This may have consequences for healing after the surgical and non-surgical phase of periodontal therapy. Moreover, the affect alleles are common in the general population with >10% frequency.

A limitation of the  $G \times G$  interaction study was the limited number of cases, which puts restraints on the significance of the  $p$ -value. Likewise, the  $G \times G$  interaction indicated a significance of  $p < .01$ , which was not significant after Bonferroni correction. Therefore, the  $G \times G$  analysis suggested an interaction but did not prove it. However, we consider that the effects of *CTD-2353F22.1* upregulation on genes and gene sets that correlate with the functions of *SIGLEC5* and *PLG* are not chance observations but confirm our results. Another limitation is that the OR of the  $G \times G$  interaction cannot be interpreted as a distinct effect size. Instead, it indicates an effect stronger than the additive effects of the individual risk alleles. Another limitation was the explanatory power of the gene-set enrichment analysis, indicated by an  $AUC \leq 0.71$ . However, lncRNAs are part of complex regulatory units that make a strong effect of a single

lncRNA unlikely (Statello et al., 2021). Another limitation of our study was that we performed genome-wide expression profiling and reporter gene activity in HeLa cells and not in cells that express *CTD-2353F* at the highest levels in nature. We chose HeLa cells because of the high transfection efficiency, which improves the sensitivity of these experiments by reducing confounding from untransfected cells. However, we found that the expression ratio of *CTD-2353F.1* isoforms in CRISPR activated HeLa cells is equal to that in B cells. Therefore, we consider the results as valid. Additionally, the lncRNA transcripts were induced by CRISPRa in HeLa cells in the same ratio as observed in primary B cells. This showed that CRISPR did not introduce a bias on the native expression ratio.

We further gave evidence that rs1122900 is a functional variant by showing allele-specific reporter gene activity and PRDM14 binding. PRDM14 is a transcription factor that plays an important role in the regulation of self-renewal of cells and enhances the efficiency of re-programming human fibroblasts (Chia et al., 2010). A limitation was that we did not validate binding of PRDM14 at rs1122900 in the native chromatin context by ChIP-seq. We also noticed that GTEx data showed reduced expression of *CTD-2353F22.1* in blood in the background of the reference rs122900-A allele. In contrast to this

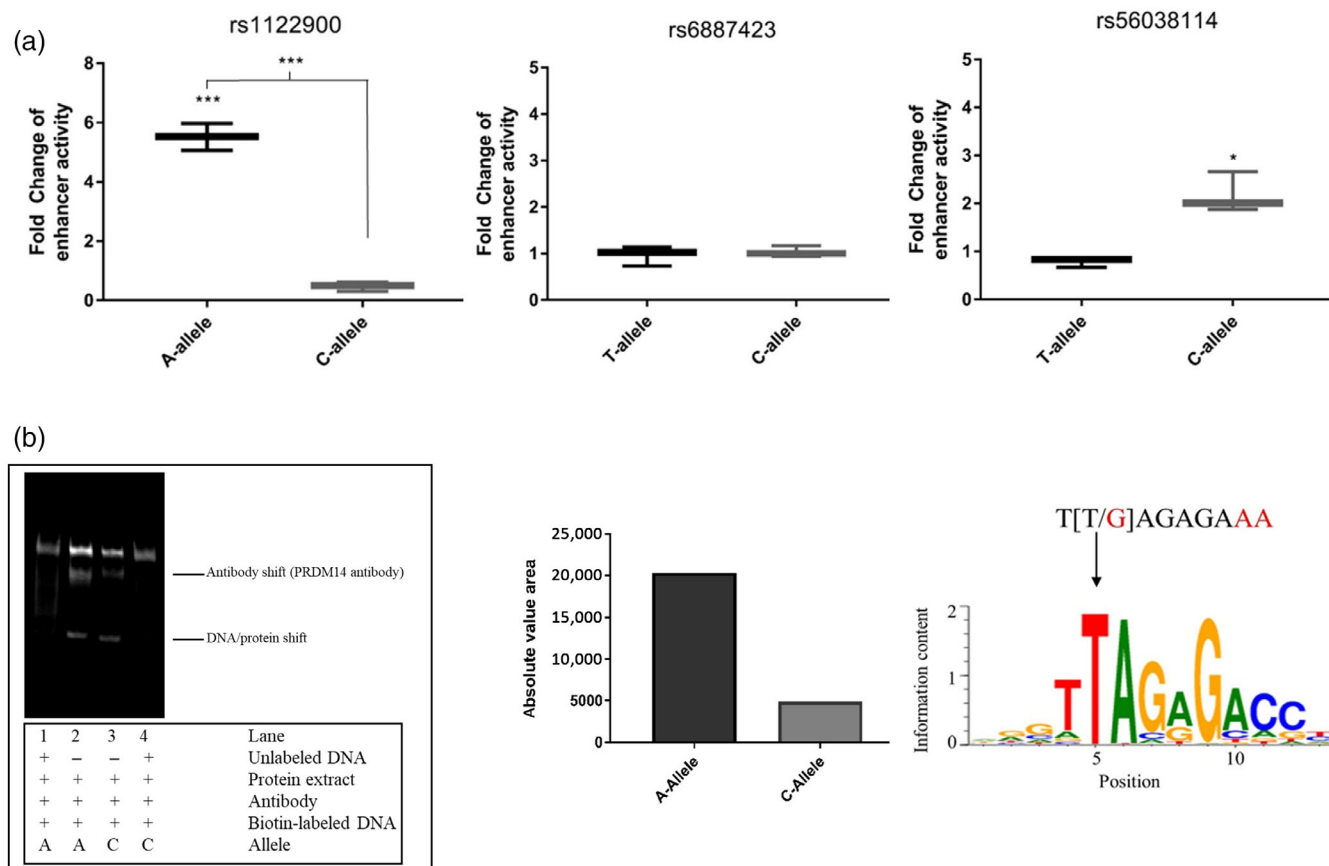


**FIGURE 5** Luciferase reporter gene assays and antibody electrophoretic mobility shift assay (EMSA) indicate rs1122900 as a putative functional single-nucleotide polymorphism with PRDM14 binding site. (a) The 146 bp DNA sequence spanning rs1122900 showed allele-specific enhancer activity in HeLa cells. In the background of the reference, A-allele luciferase activity was 5.5-fold higher compared with the alternative C-allele ( $p = .0003$ ), which showed no upregulation. The difference between both alleles was significant with  $p = .0005$  (left). The 143 bp DNA sequence spanning rs6887423 showed no allele-specific effects on luciferase activity (middle). The 147 bp DNA sequence with the reference rs56038114-T allele did not increase the luciferase activity effect in HeLa cells. The alternative C-allele showed 2.2-fold upregulation of the reporter gene with  $p = .01$  (right). \* $p < .05$ , \*\* $p < .005$  and \*\*\* $p \leq .0005$ . (b) PRDM14-antibody EMSA performed with rs1122900 allele-specific oligonucleotide probes and nuclear protein extract from Raji cells. Binding of PRDM14-antibody to allele-specific probes is shown in lanes 2 and 3. Probes with the effect C-allele abrogated antibody binding compared with probes with the reference A-allele. Unlabeled DNA was added to verify that the band-shift was antibody specific in lanes 1 and 4 (left). Absolute value area of the PRDM14 antibody-specific band. The rs1122900 C-allele reduced PRDM14 binding by 76% compared with the A-allele (middle). PWM of the transcription factor binding sites for PRDM14 indicates that the PRDM14 binding motif has 89% matrix similarity with the DNA sequence at the A-allele (right).

observation, our reporter gene showed increased luciferase activity with the A-allele in HeLa cells. Although speculative, it is possible that in vivo eQTLs differ from in vitro reporter gene activity, because of the small length of the tested candidate DNA sequence or differences between clones of a single cell type and complex cell type composition of whole blood. Correspondingly to the GTEx data, a repressive role of PRDM14 was reported (Tsuneyoshi et al., 2008; Chia et al., 2010; Chan et al., 2013) and it is conceivable that PRDM14 binding at the A-allele that we observed in the EMSA experiments may repress *CTD-2353F22.1* transcription in vivo.

In conclusion, the current G×G interaction analysis revealed interrelations of the genetic associations at *SIGLEC5* and *PLG* with the lncRNA *CTD-2353F22.1*. Our results showed that this lncRNA has a role in the regulation of wound healing and vascularization and imply an important role of these processes in the etiopathogenesis of periodontitis.

## AUTHOR CONTRIBUTIONS

All authors contributed to drafting and revising the work critically, gave final approval of the published version and are accountable for all aspects of the work. Ricarda Müller, Sandra Freitag-Wolf and Arne S. Schaefer contributed to the conception and design of the work, data acquisition, analysis and interpretation of data; January Weiner 3rd, Avneesh Chopra and Tugba Top contributed to data acquisition, analysis and interpretation of data and Henrik Dommisch contributed to interpretation of data.

## ACKNOWLEDGEMENTS

This work was funded by the German Research Foundation by grants given to AS (SCHA1582 5-1) and SFW (Clusterlab XI EXC 306/2), and by the medical faculty of Christian-Albrecht University of Kiel (K 126 202) with a grant given to SFW. All authors gave their final approval

and agreed to be accountable for all aspects of the work. The authors declare no potential conflicts of interest with respect to the authorship and/or publication of this article. All authors gave their final approval and agreed to be accountable for all aspects of the work. Open Access funding enabled and organized by Projekt DEAL.

## CONFLICT OF INTEREST

The authors declare no conflicts of interest.

## DATA AVAILABILITY STATEMENT

The data that support the findings of this study are available on request from the corresponding author. The data are not publicly available due to privacy or ethical restrictions.

## ETHICS STATEMENT

The institutional review boards of the Christian-Albrechts University, Kiel and Charité—Universitätsmedizin, Berlin approved the study. Participants' completion of the questionnaires constituted informed consent.

## ORCID

Henrik Dommisch  <https://orcid.org/0000-0003-1043-2651>

Arne S. Schaefer  <https://orcid.org/0000-0001-5816-6765>

## REFERENCES

- 1000 Genomes Project Consortium, Auton, A., Brooks, L. D., Durbin, R. M., Garrison, E. P., Kang, H. M., Korbel, J. O., Marchini, J. L., McCarthy, S., McVean, G., & Abecasis, G. R. (2015). A global reference for human genetic variation. *Nature*, 526(7571), 68–74. <https://doi.org/10.1038/nature15393>
- Abugessaisa, I., Ramilowski, J. A., Lizio, M., Severin, J., Hasegawa, A., Harshbarger, J., Kondo, A., Noguchi, S., Yip, C. W., Ooi, J. L. C., Tagami, M., Hori, F., Agrawal, S., Hon, C. C., Cardon, M., Ikeda, S., Ono, H., Bono, H., Kato, M., ... Kasukawa, T. (2021). FANTOM enters 20th year: Expansion of transcriptomic atlases and functional annotation of non-coding RNAs. *Nucleic Acids Research*, 49(D1), D892–D898. <https://doi.org/10.1093/nar/gkaa1054>
- Aleknyte-Resch, M., Freitag-Wolf, S., International Inflammatory Bowel Disease Genetics, C., Schreiber, S., Krawczak, M., & Dempfle, A. (2020). Case-only analysis of gene-gene interactions in inflammatory bowel disease. *Scandinavian Journal of Gastroenterology*, 55(8), 897–906. <https://doi.org/10.1080/00365521.2020.1790646>
- Boyle, E. A., Li, Y. I., & Pritchard, J. K. (2017). An expanded view of complex traits: From polygenic to omnigenic. *Cell*, 169(7), 1177–1186. <https://doi.org/10.1016/j.cell.2017.05.038>
- Caton, J. G., Armitage, G., Berglundh, T., Chapple, I. L. C., Jepsen, S., Kornman, K. S., Mealey, B. L., Papapanou, P. N., Sanz, M., & Tonetti, M. S. (2018). A new classification scheme for periodontal and peri-implant diseases and conditions – Introduction and key changes from the 1999 classification. *Journal of Clinical Periodontology*, 45-(Suppl 20), S1–S8. <https://doi.org/10.1111/jcpe.12935>
- Chan, Y. S., Goke, J., Lu, X., Venkatesan, N., Feng, B., Su, I. H., & Ng, H. H. (2013). A PRC2-dependent repressive role of PRDM14 in human embryonic stem cells and induced pluripotent stem cell reprogramming. *Stem Cells*, 31(4), 682–692. <https://doi.org/10.1002/stem.1307>
- Chen, G. Y., Tang, J., Zheng, P., & Liu, Y. (2009). CD24 and Siglec-10 selectively repress tissue damage-induced immune responses. *Science*, 323(5922), 1722–1725. <https://doi.org/10.1126/science.1168988>
- Chia, N. Y., Chan, Y. S., Feng, B., Lu, X., Orlov, Y. L., Moreau, D., Kumar, P., Yang, L., Jiang, J., Lau, M. S., Huss, M., Soh, B. S., Kraus, P., Li, P., Lufkin, T., Lim, B., Clarke, N. D., Bard, F., & Ng, H. H. (2010). A genome-wide RNAi screen reveals determinants of human embryonic stem cell identity. *Nature*, 468(7321), 316–320. <https://doi.org/10.1038/nature09531>
- Chopra, A., Mueller, R., Weiner, J., 3rd, Rosowski, J., Dommisch, H., Grohmann, E., & Schaefer, A. S. (2021). BACH1 binding links the genetic risk for severe periodontitis with ST8SIA1. *Journal of Dental Research*, 101, 93–101. <https://doi.org/10.1177/00220345211017510>
- Chu, C., Qu, K., Zhong, F. L., Artandi, S. E., & Chang, H. Y. (2011). Genomic maps of long noncoding RNA occupancy reveal principles of RNA-chromatin interactions. *Molecular Cell*, 44(4), 667–678. <https://doi.org/10.1016/j.molcel.2011.08.027>
- Drake, T. A., Morrissey, J. H., & Edgington, T. S. (1989). Selective cellular expression of tissue factor in human tissues. Implications for disorders of hemostasis and thrombosis. *The American Journal of Pathology*, 134(5), 1087–1097.
- eGTEx Project. (2017). Enhancing GTEx by bridging the gaps between genotype, gene expression, and disease. *Nature Genetics*, 49(12), 1664–1670. <https://doi.org/10.1038/ng.3969>
- Fay, W. P., Parker, A. C., Condrey, L. R., & Shapiro, A. D. (1997). Human plasminogen activator inhibitor-1 (PAI-1) deficiency: Characterization of a large kindred with a null mutation in the PAI-1 gene. *Blood*, 90(1), 204–208.
- Freitag-Wolf, S., Munz, M., Junge, O., Graetz, C., Jockel-Schneider, Y., Staufienbiel, I., Bruckmann, C., Lieb, W., Franke, A., Loos, B. G., Jepsen, S., Dommisch, H., & Schaefer, A. S. (2021). Sex-specific genetic factors affect the risk of early-onset periodontitis in Europeans. *Journal of Clinical Periodontology*, 48(11), 1404–1413. <https://doi.org/10.1111/jcpe.13538>
- Freitag-Wolf, S., Munz, M., Wiehe, R., Junge, O., Graetz, C., Jockel-Schneider, Y., Staufienbiel, I., Bruckmann, C., Lieb, W., Franke, A., Loos, B. G., Jepsen, S., Dommisch, H., & Schaefer, A. S. (2019). Smoking modifies the genetic risk for early-onset periodontitis. *Journal of Dental Research*, 98(12), 1332–1339. <https://doi.org/10.1177/0022034519875443>
- Gauderman, W. J. (2002). Sample size requirements for matched case-control studies of gene-environment interaction. *Statistics in Medicine*, 21(1), 35–50. <https://doi.org/10.1002/sim.973>
- Jankun, J., Aleem, A. M., Selman, S. H., Skrzypczak-Jankun, E., Lysiak-Szydlowska, W., Grafos, N., Fryer, H. J. L., & Greenfield, R. S. (2007). Highly stable plasminogen activator type one (VLHL PAI-1) protects fibrin clots from tissue plasminogen activator-mediated fibrinolysis. *International Journal of Molecular Medicine*, 20(5), 683–687.
- Lee, M. H., Vosburgh, E., Anderson, K., & McDonagh, J. (1993). Deficiency of plasma plasminogen activator inhibitor 1 results in hyperfibrinolytic bleeding. *Blood*, 81(9), 2357–2362.
- Lizio, M., Harshbarger, J., Shimoji, H., Severin, J., Kasukawa, T., Sahin, S., Abugessaisa, I., Fukuda, S., Hori, F., Ishikawa-Kato, S., Mungall, C. J., Arner, E., Baillie, J. K., Bertin, N., Bono, H., de Hoon, M., Diehl, A. D., Dimont, E., Freeman, T. C., ... FANTOM consortium. (2015). Gateways to the FANTOM5 promoter level mammalian expression atlas. *Genome Biology*, 16, 22. <https://doi.org/10.1186/s13059-014-0560-6>
- Munz, M., Richter, G. M., Loos, B. G., Jepsen, S., Divaris, K., Offenbacher, S., Teumer, A., Holtfreter, B., Kocher, T., Bruckmann, C., Jockel-Schneider, Y., Graetz, C., Ahmad, I., Staufienbiel, I., van der Velde, N., Uitterlinden, A. G., de Groot, L. C. P. G. M., Wellmann, J., Berger, K., ... Schaefer, A. S. (2019). Meta-analysis of genome-wide association studies of aggressive and chronic periodontitis identifies two novel risk loci. *European Journal of Human Genetics*, 27(1), 102–113. <https://doi.org/10.1038/s41431-018-0265-5>
- Munz, M., Willenborg, C., Richter, G. M., Jockel-Schneider, Y., Graetz, C., Staufienbiel, I., Wellmann, J., Berger, K., Krone, B., Hoffmann, P., van der Velde, N., Uitterlinden, A. G., de Groot, L. C. P. G. M., Sawalha, A. H., Direskeneli, H., Saruhan-Direskeneli, G., Guzeldemir-

- Akcakanat, E., Keceli, H. G., Laudes, M., ... Schaefer, A. S. (2017). A genome-wide association study identifies nucleotide variants at SIGLEC5 and DEFA1A3 as risk loci for periodontitis. *Human Molecular Genetics*, 26, 2577–2588. <https://doi.org/10.1093/hmg/ddx151>
- Opneja, A., Kapoor, S., & Stavrou, E. X. (2019). Contribution of platelets, the coagulation and fibrinolytic systems to cutaneous wound healing. *Thrombosis Research*, 179, 56–63. <https://doi.org/10.1016/j.thromres.2019.05.001>
- Piegorsch, W. W., Weinberg, C. R., & Taylor, J. A. (1994). Non-hierarchical logistic models and case-only designs for assessing susceptibility in population-based case-control studies. *Statistics in Medicine*, 13(2), 153–162. <https://doi.org/10.1002/sim.4780130206>
- Planus, E., Barlovatz-Meimon, G., Rogers, R. A., Bonavaud, S., Ingber, D. E., & Wang, N. (1997). Binding of urokinase to plasminogen activator inhibitor type-1 mediates cell adhesion and spreading. *Journal of Cell Science*, 110(Pt 9), 1091–1098.
- Providence, K. M., Higgins, S. P., Mullen, A., Battista, A., Samarakoon, R., Higgins, C. E., Wilkins-Port, C. E., & Higgins, P. J. (2008). SERPINE1 (PAI-1) is deposited into keratinocyte migration “trails” and required for optimal monolayer wound repair. *Archives of Dermatological Research*, 300(6), 303–310. <https://doi.org/10.1007/s00403-008-0845-2>
- Shungin, D., Haworth, S., Divaris, K., Agler, C. S., Kamatani, Y., Keun Lee, M., Grinde, K., Hindy, G., Alaraudanjoki, V., Pesonen, P., Teumer, A., Holtfreter, B., Sakaue, S., Hirata, J., Yu, Y. H., Ridker, P. M., Giulianini, F., Chasman, D. I., Magnusson, P. K. E., ... Johansson, I. (2019). Genome-wide analysis of dental caries and periodontitis combining clinical and self-reported data. *Nature Communications*, 10(1), 2773. <https://doi.org/10.1038/s41467-019-10630-1>
- Silva, L. M., Doyle, A. D., Greenwell-Wild, T., Dutzan, N., Tran, C. L., Abusleme, L., Juang, L. J., Leung, J., Chun, E. M., Lum, A. G., Agler, C. S., Zuazo, C. E., Sibree, M., Jani, P., Kram, V., Martin, D., Moss, K., Lionakis, M. S., Castellino, F. J., ... Moutsopoulos, N. M. (2021). Fibrin is a critical regulator of neutrophil effector function at the oral mucosal barrier. *Science*, 374(6575), eabl5450. <https://doi.org/10.1126/science.abl5450>
- Simantov, R., & Silverstein, R. L. (2003). CD36: A critical anti-angiogenic receptor. *Frontiers in Bioscience*, 8, s874–s882. <https://doi.org/10.2741/1168>
- Simone, T. M., Higgins, C. E., Czekay, R. P., Law, B. K., Higgins, S. P., Archambeault, J., Kutz, S. M., & Higgins, P. J. (2014). SERPINE1: A molecular switch in the proliferation-migration dichotomy in wound-“activated” keratinocytes. *Advances in Wound Care*, 3(3), 281–290. <https://doi.org/10.1089/wound.2013.0512>
- Statello, L., Guo, C. J., Chen, L. L., & Huarte, M. (2021). Gene regulation by long non-coding RNAs and its biological functions. *Nature Reviews. Molecular Cell Biology*, 22(2), 96–118. <https://doi.org/10.1038/s41580-020-00315-9>
- Streit, M., Velasco, P., Riccardi, L., Spencer, L., Brown, L. F., Janes, L., Lange-Asschenfeldt, B., Yano, K., Hawighorst, T., Iruela-Arispe, L., & Detmar, M. (2000). Thrombospondin-1 suppresses wound healing and granulation tissue formation in the skin of transgenic mice. *The EMBO Journal*, 19(13), 3272–3282. <https://doi.org/10.1093/emboj/19.13.3272>
- Suhre, K., Arnold, M., Bhagwat, A. M., Cotton, R. J., Engelke, R., Raffler, J., Sarwath, H., Thareja, G., Wahl, A., DeLisle, R., Gold, L., Pezer, M., Lauc, G., el-Din Selim, M. A., Mook-Kanamori, D. O., al-Dous, E. K., Mohamoud, Y. A., Malek, J., Strauch, K., ... Graumann, J. (2017). Connecting genetic risk to disease end points through the human blood plasma proteome. *Nature Communications*, 8, 14357. <https://doi.org/10.1038/ncomms14357>
- Takekawa, M., & Saito, H. (1998). A family of stress-inducible GADD45-like proteins mediate activation of the stress-responsive MTK1/MEKK4 MAPKKK. *Cell*, 95(4), 521–530. [https://doi.org/10.1016/s0092-8674\(00\)81619-0](https://doi.org/10.1016/s0092-8674(00)81619-0)
- Timpson, N. J., Greenwood, C. M. T., Soranzo, N., Lawson, D. J., & Richards, J. B. (2018). Genetic architecture: The shape of the genetic contribution to human traits and disease. *Nature Reviews. Genetics*, 19(2), 110–124. <https://doi.org/10.1038/nrg.2017.101>
- Tonnesen, M. G., Feng, X., & Clark, R. A. (2000). Angiogenesis in wound healing. *The Journal of Investigative Dermatology. Symposium Proceedings*, 5(1), 40–46. <https://doi.org/10.1046/j.1087-0024.2000.00014.x>
- Tran, H., Brunet, A., Grenier, J. M., Datta, S. R., Fornace, A. J., Jr., DiStefano, P. S., Chiang, L. W., & Greenberg, M. E. (2002). DNA repair pathway stimulated by the forkhead transcription factor FOXO3a through the Gadd45 protein. *Science*, 296(5567), 530–534. <https://doi.org/10.1126/science.1068712>
- Tsuneyoshi, N., Sumi, T., Onda, H., Nojima, H., Nakatsuji, N., & Suemori, H. (2008). PRDM14 suppresses expression of differentiation marker genes in human embryonic stem cells. *Biochemical and Biophysical Research Communications*, 367(4), 899–905. <https://doi.org/10.1016/j.bbrc.2007.12.189>
- Visscher, P. M., Wray, N. R., Zhang, Q., Sklar, P., McCarthy, M. I., Brown, M. A., & Yang, J. (2017). 10 Years of GWAS discovery: Biology, function, and translation. *American Journal of Human Genetics*, 101(1), 5–22. <https://doi.org/10.1016/j.ajhg.2017.06.005>
- Westra, H. J., Peters, M. J., Esko, T., Yaghootkar, H., Schurmann, C., Kettunen, J., Christiansen, M. W., Fairfax, B. P., Schramm, K., Powell, J. E., Zernakova, A., Zernakova, D. V., Veldink, J. H., van den Berg, L., Karjalainen, J., Withoff, S., Uitterlinden, A. G., Hofman, A., Rivadeneira, F., ... Franke, L. (2013). Systematic identification of trans eQTLs as putative drivers of known disease associations. *Nature Genetics*, 45(10), 1238–1243. <https://doi.org/10.1038/ng.2756>
- Wray, N. R., Wijmenga, C., Sullivan, P. F., Yang, J., & Visscher, P. M. (2018). Common disease is more complex than implied by the core gene omnigenic model. *Cell*, 173(7), 1573–1580. <https://doi.org/10.1016/j.cell.2018.05.051>

## SUPPORTING INFORMATION

Additional supporting information can be found online in the Supporting Information section at the end of this article.

**How to cite this article:** Müller, R., Freitag-Wolf, S., Weiner, J. 3rd, Chopra, A., Top, T., Dommisch, H., & Schaefer, A. S. (2023). Case-only design identifies interactions of genetic risk variants at SIGLEC5 and PLG with the lncRNA CTD-2353F22.1 implying the importance of periodontal wound healing for disease aetiology. *Journal of Clinical Periodontology*, 50(1), 90–101. <https://doi.org/10.1111/jcpe.13712>